2564 *Macromolecules* **2010**, *43*, 2564–2573
DOI: 10.1021/ma902623u

Macromolecules
ARTICLE

On the Influence of Topological Catenation and Bonding Constraints on Ring Polymers

Manfred Bohn,*,† Dieter W. Heermann,† Odilon Lourenço,‡ and Claudette Cordeiro‡

†*Institute of Theoretical Physics, University of Heidelberg, Philosophenweg 19, D-69120 Heidelberg, Germany, and* ‡*Instituto de Fisica, Universidade Federal Fluminense, 24.210.340-Niteroi-RJ, Brazil*

Received September 15, 2009; Revised Manuscript Received February 4, 2010

ABSTRACT: The ring structure of certain polymers in nature, like proteins and DNA indicates a benefit compared with the linear form. Transcriptional regulation in higher eukaryotes is maintained among others by the formation of chromatin loops. Experimental studies revealed that different chromosomes as well as chromatin regions on one single chromosome tend to be segregated into distinct territories. Here we study a system of two rings in both catenane and bonded topology as a toy model for the influence of loops and topological constraints on the polymers' conformational properties. Athermal Monte Carlo simulations reveal that the mean square radius of gyration $\langle R_{gyr}^2 \rangle$ of catenated or bonded rings follows a similar scaling exponent as isolated rings, which in turn is close to the value of $\nu \approx 0.588$ for a self-avoiding walk. However, the effective segment length is larger for catenated rings, reflecting the swelling of the polymers. The shape of catenated and bonded rings, in contrast, shows pronounced differences even in the limit of infinite chain length. We observe a strong tendency toward segregation for the bonded topology in comparison with a similar ring−linear and linear−linear system. The orientation of the rings' gyration ellipsoids is slightly perpendicular, trying to minimize the overlap area. These findings indicate that loops might play an important role in the entropy-driven segregation of chromatin.

Introduction

Ring polymers differ from linear polymers in that the end points are connected to a cyclic form. The investigation of these polymers is not of pure theoretical interest. In fact, they are abundant in nature. First evidence of certain DNA molecules to occur in a ring shape has been found as early as 1962 by ultracentrifugation.[1] One year later, experimental results indicated that the double-stranded DNA of the polyoma virus exists in a closed cyclic structure.[2,3] Nowadays, it is clear that cyclic ring polymers are quite abundant in organisms and the ring structure seems to play an important role in the genomic function of organisms. Among others, circular DNA is found in bacteria, viruses, as well as in eukaryotic cells, where the mitochondrial DNA has a cyclic structure. Furthermore, loops have shown to be an ubiquitous feature of chromatin organization in higher eukaryotes.[4,5] These loops in turn can be viewed as ring polymers, although it needs to be stressed that they are not isolated from the rest of the chain.

The conformational properties of isolated ring polymers have been extensively studied in the past by theory and simulations[6−8] both with and without excluded volume interactions. It was shown that self-avoiding polymer rings follow the same scaling behavior as isolated linear polymers in the limit of infinite chain length $N \rightarrow \infty$ concerning its static properties.[9] A lot of studies are devoted to the question of how the scaling behavior of the radius of gyration $R_{gyr}(N)$ changes when isolated ring polymers are constrained to a fixed topology, that is, knot type. It has been proposed in an analytical argument[10] that topological constraints alone induce the same scaling as excluded volume interactions, that is

$$R_{gyr}{}^2(N) \approx N^{2\nu} \tag{1}$$

*Corresponding author. E-mail: bohn@tphys.uni-heidelberg.de.

Later, it was shown[11] that the size of a ring polymer without excluded volume in a quenched topology displays a crossover from a random-walk type of scaling to a self-avoiding walk type of scaling for larger chain lengths. This result was later confirmed by numerical studies for trivially knotted ring polymers.[12]

A system of several rings can display a variety of different topological states. Rings can be either noncatenated or catenated, the degree of catenation varying. Brown et al.[13] studied the influence of topological constraints of isolated rings and rings in a melt with excluded volume and came up with the conclusion that topological constraints influence the isolated chain behavior only marginally, whereas rings in a melt exhibit dramatic changes by turning on topological constraints. This is in agreement with a study by Müller,[14] showing that noncatenated rings in a melt become compact with a scaling exponent of $\nu \approx 0.39$. This compactification, not detected for, for example, linear polymers, indicates a strong effect of topology. The scaling exponent found is consistent with a Flory-type of argument[15] yielding $\nu = 2/5$. Further computational studies led to the proposal that the scaling exponent is a crossover effect asymptotically moving toward a behavior similar to compact lattice animals in a self-consistent network of topological constraints,[16] a result that has been recently confirmed.[17] Summarizing these results, a general conclusion emerging is that topological constraints introduced by the cyclic structure into the problem of polymeric conformations alter conformational properties in a melt of rings quite drastically.

Whereas many studies had their focus predominantly on the topological effects of the noncatenation constraint in a melt, the study of catenated or bonded rings can yield further insight into their topological interactions. Such rings are held relatively close together by means of the constraint; therefore, they can be used as an ideal model for examining interactions between them. Similar approaches have been used to study the topological origin of chromosome territories in other publications.[18,19] The catenane

 Published on Web 02/15/2010

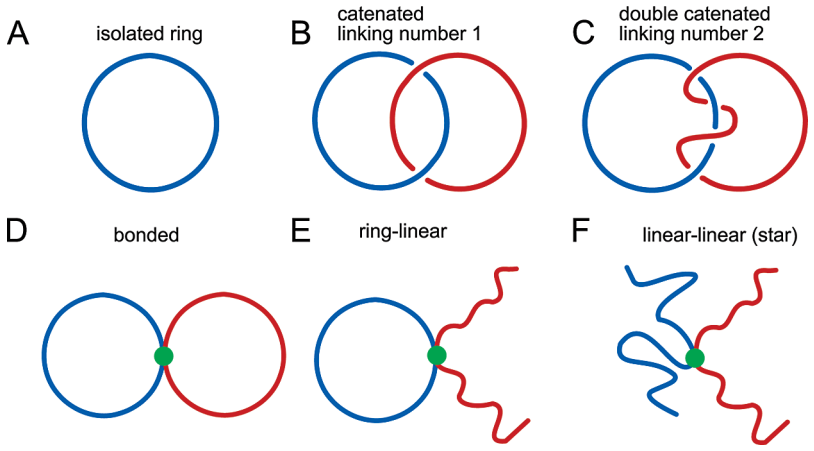

Figure 1. Different ring topologies used in this study. (A) Isolated rings are used as the reference ensemble. Two types of linked two-ring conformations are studied: (B) Catenated rings with a Hopf link, that is, the simplest nontrivial link type with Gauss linking number $\Phi = 1$, and (C) double-catenated rings with $\Phi = 2$. (D) Rings without catenation, but with two monomers bonded to each other are studied. (E) Ring-linear and (F) star-shaped linear−linear conformations are simulated for purposes of comparison.

topology is common in nature. The equilibrium distribution of topological states of DNA was determined by random cyclization experiments of linear DNA, resulting in a broad distribution of linking numbers.[20] Later, it was shown that this equilibrium distribution is greatly modified by the activity of type II DNA topoisomerase, an enzyme that allows us to release topological constraints.[21] Recently, the effect of catenation on protein-folding stability has been studied.[22] Although chromatin is not circular inside the human interphase nucleus, there is now abundant experimental evidence that transcriptional regulation is accomplished by the formation of polymeric loops.[4,23] Transcription factors are assumed to have the possibility of aggregating inside the nucleus, building transcription hubs or factories[24] where genes can bind to, therefore effectuating an enhancement of the expression level. The intervening DNA then has to loop out. Such looping has recently been proposed to have a major impact on the observed segregation of chromosomes.[25] We want to emphasize that the present study does not consider chromosomes in their complexity, but the general physical properties of ring polymers. However, similar effects can be expected to be present in transcription factories, where loops come close together. The existence of several loops might even lead to a stronger effect, as has been observed for a melt of loops.[17]

The scope of this study is to deepen the understanding of the ring structure accompanied by the induced topological state on the conformational properties of the polymers involved. To achieve this, we study both isolated ring polymers as well as two-ring conformations with a fixed topology. The topological state of two ring polymers with paths C_1 and C_2 can be characterized by the Gauss linking number[26]

$$\Phi = \frac{1}{4\pi}\oint_{C_1}\oint_{C_2}\frac{\langle d\mathbf{r}_1 \times d\mathbf{r}_2, \mathbf{r}_1 - \mathbf{r}_2\rangle}{|\mathbf{r}_1 - \mathbf{r}_2|^3} \qquad (2)$$

It has to be noted that a one-to-one correspondence between the Gauss link invariant and the topological state cannot be established. Three different topologies are investigated exemplarily: simple catenated rings (the Hopf link, $\Phi = 1$), double-catenated rings ($\Phi = 2$), and rings that are noncatenated ($\Phi = 0$) but bonded together at one monomer. Whereas the first two systems are interesting for DNA and protein catenanes, the latter resembles chromatin loops assembled in transcription hubs. Effects of catenation have been analyzed concerning dimensionality by Sikorski[27] for rings up to $N = 800$. He conjectured that the dimensions and shape of a catenated polymer ring approach the values of an isolated ring in the limit of infinite chain length. However, a stringent analysis of the changes in dimensionality as well as shape has not been undertaken. In this study we focus on three points: First, the changes in the dimensions characterized by the radius of gyration and the mean square ring diameter induced by the existence of a second ring are investigated. We carefully analyze whether the scaling exponent, ν, is different in the limit of infinite chain length, $N \rightarrow \infty$. Second, we ask whether rings in a catenated or bonded topology display a different shape than their linear counterparts. In contrast with Sikorski's conjecture, we find pronounced differences in the shape of isolated rings compared with catenated or bonded rings, even in the limit of large chain length. Finally, especially with respect to the biological systems, we ask the question of whether such a two-ring system is able to intermingle freely or whether there is a tendency to segregate. Comparison with corresponding linear counterparts provides us with evidence of topological constraints and looping indeed lead to a more ordered and compartmentalized state.

The article is organized as follows: In the next section, we describe the simulation method as well as the sampling procedure. We then present results for the dimensions of isolated rings as well as the two-ring topologies studied. Afterward, the influence of the topological constraints on the shape of the rings is investigated. In the last two sections, we elaborate on their tendency to intermingle or segregate as well as their mutual alignment.

Computational Model

To investigate the influence of topology on the properties of ring polymers, a model system of two ring conformations is simulated in a fixed topological state with excluded volume interactions. The topologies studied are displayed in Figure 1. Dimensionality and shape of isolated rings (Figure 1A) are calculated as a reference. The catenane topology is studied using the two simplest link types: First, the Hopf link with a Gauss linking number $\Phi = 1$; that is, chain 1 passes through the surface of chain 2 exactly once (Figure 1B). Second, double-catenated rings with a Gauss linking number $\Phi = 2$ (Figure 1C). It is to be stressed at this point that we do not sample the complete ensemble of rings with Gauss linking number one or two, as the correspondence of linking number and link topology is not one-to-one. Rather we sample the specific link types shown in Figure 1 as we are interested in the influence of the topological constraints rather than the properties of the Gauss linking number. Noncatenated rings with $\Phi = 0$ are set up such that they are connected at one point, this connection persisting during the time of simulations

(Figure 1D). To deepen the insight into entropic and topological effects of ring closure, we study the behavior of bonded noncatenated chains where one or both rings are cut to make a ring-linear or linear−linear star-shaped system (Figure 1E,F).

Monte Carlo Algorithm. We use a coarse-grained lattice Monte Carlo method[28] to simulate ring polymers. We fully take into account excluded volume interactions as well as topological constraints; that is, no bond crossings are allowed. These can be easily implemented with the bond fluctuation model,[29] which we use here. The coarse-grained monomers are residing in the center of the unit cubes of a simple cubic lattice and occupy all eight vertices of this unit cube. Each monomer is allowed to fluctuate freely as long as the connection with its two neighbors, to which it is bonded, and therefore the connectivity of the chain is preserved. The lattice constant is taken to be unity, and all measures of length in the following are given in multiples of the lattice constant. The length of the bonds between two neighboring monomers are allowed to fluctuate in contrast with a model on a simple cubic lattice (e.g., the Verdier−Stockmayer algorithm[30]). Excluded volume interactions are easily implemented in this lattice model; their calculation reduces to a test whether a certain lattice site is already occupied or not. As one monomer fills eight lattice sites, the nearest distance between two monomers is 2. Care has to be taken concerning the preservation of topology. For our simulation, this is a crucial point, because we want to see effects of the topological constraints. However, a fixed topology is accomplished automatically by putting restrictions on the allowed bond vectors and moves. It can be shown[31] that an allowed set $\mathscr{B}$ of 108 bond vectors, where the bond length can take on any of the values 2, $\sqrt{5}$, $\sqrt{6}$, 3, and $\sqrt{10}$, is enough to maintain the topological state of the ring polymers when only local moves are applied. Local moves imply all moves where one monomer is moved at a time maximally to one of its six nearest neighbors, that is, the change in distance is $\delta r \in \{0, \pm 1\}$.

The chain is propagated via the Metropolis Monte Carlo algorithm;[28] that is, a new conformation is proposed and accepted with a probability of $\min\{1, \exp(-\beta\ \delta U)\}$. The proposal of a new conformation is based on randomly selecting one monomer, followed by randomly selecting one of the nearest neighbors' positions on the lattice. The energy calculation of our athermal simulations is quite easy: If the lattice site is already occupied or one of the two bond vectors does not belong to the set $\mathscr{B}$ of the allowed bond vectors, then the change in energy is $\delta U = +\infty$, and the proposed conformation is rejected, otherwise the change in energy is $\delta U = 0$, resulting in an acceptance of the new conformation. In the following, one Monte Carlo step (1 MCS) is defined as the number of attempted moves, where on average, each monomer has performed one trial move.

Data Acquisition and Autocorrelation Times. The linear dimension of the simulation box is chosen between $L = 256$ and $L = 800$, ensuring L to be larger than the typical size of the polymer, $L \gg (\langle R_{gyr}^2 \rangle)^{1/2}$. Although periodic boundary conditions are used, the algorithm keeps track of unfolded coordinates so that the monomer can diffuse freely through space. The choice of the size of the simulation box is guided by the attempt to minimize the probability that monomers, which are far apart in terms of unfolded coordinates touching each other inside the simulation box, while at the same time keeping the effort in memory usage during the simulation reasonable. By using this method, the chains do not feel the simulation box or the periodic boundaries.

Because the topology is kept fixed during the simulation run by virtue of the algorithm chosen, the initial conformation has to be set up with the correct topology, that is, those displayed in Figure 1. The conformations are then propagated in a manner equivalent to real polymer rings, that is, by continuous chain deformations without bond crossings. We demand each ring to be unknotted. Simple catenated rings have to pass through each other's surface spanned by their paths exactly once. The initial conformation for isolated chains is set up as a rectangle in the xy plane; if the chain length is too large with respect to the lattice size, then small humps in the z direction are created. For the simple catenated ring conformations, the second ring is positioned perpendicularly to the first one and shifted by 2 lattice units. Similarly, double-catenated rings are created. In the case of noncatenated bonded rings, two rings are set up comparable to the isolated case at different z values and connected at one site.

The bond fluctuation method has been invented among others to overcome ergodicity problems with the Verdier−Stockmayer algorithm. It has been successfully applied to both linear polymers as well as ring polymers[14,31] so that it can be assumed to be ergodic in both cases. To make sure that also in the case of two interlinked rings the algorithm does not get stuck, we have analyzed whether subsequent conformations are really different. No indication was found for ergodicity problems similar to the Verdier−Stockmayer algorithm. Applying only local moves with the restriction of not allowing bond crossings further ensures that the conformational space is similar to (although not continuous) to the one obtained in real polymers by continuously deforming the rings.

Because the simulation method applied here only implements local moves, one conformation emerging from another by propagating it one Monte Carlo step differs only slightly; in other words, both conformations are highly correlated. To obtain uncorrelated samples of ring conformations, we have to perform a certain number of Monte Carlo steps given by the autocorrelation or relaxation time τ.[32] We approximate τ by calculating the autocorrelation function $C(t)$ of the squared radius of gyration, $A(t) = R_{gyr}^2(t)$, from the simulation data,

$$C(t) = \frac{\langle A(t)A(0)\rangle - \langle A\rangle^2}{\langle A^2\rangle - \langle A\rangle^2}$$

Then, the integrated autocorrelation time is calculated by Sokal's windowing procedure[33] with the break condition $T \geq 10\tau_{int}(T)$. Here $\tau_{int}(T)$ is the integrated autocorrelation time, that is, the integral of $C(t)$ up to the time, T. $\tau = \tau_{int}(T^*)$ is obtained using the smallest value T^*, satisfying the break condition. Error calculations are based on considering two subsequent conformations to be independent after 5τ MCS.

Simulations are performed with chain lengths ranging from $N = 32$ to 2048. Autocorrelation times increase quadratic in the chain length, $\tau \approx aN^2$, the scaling constant being ~2.01 for isolated rings and ~2.54 for simple catenated rings. For each chain length, 8 000−80 000 independent isolated and catenated ring conformations were created. Simulations were performed on the Helics cluster at the Interdisciplinary Center for Scientific Computing (IWR) in Heidelberg and the bwGrid cluster at the University of Heidelberg.

Results

Catenation and Bonding Influences Ring Dimensions Slightly. Whereas the dimensions of linear polymers are often characterized by the mean-squared end-to-end distance $\langle R_e^2 \rangle$, which exhibits the well-known scaling law $\langle R_e^2 \rangle \approx N^{2\nu}$, this is obviously not a good measure for the size of a ring polymer, where end points are not defined at all.

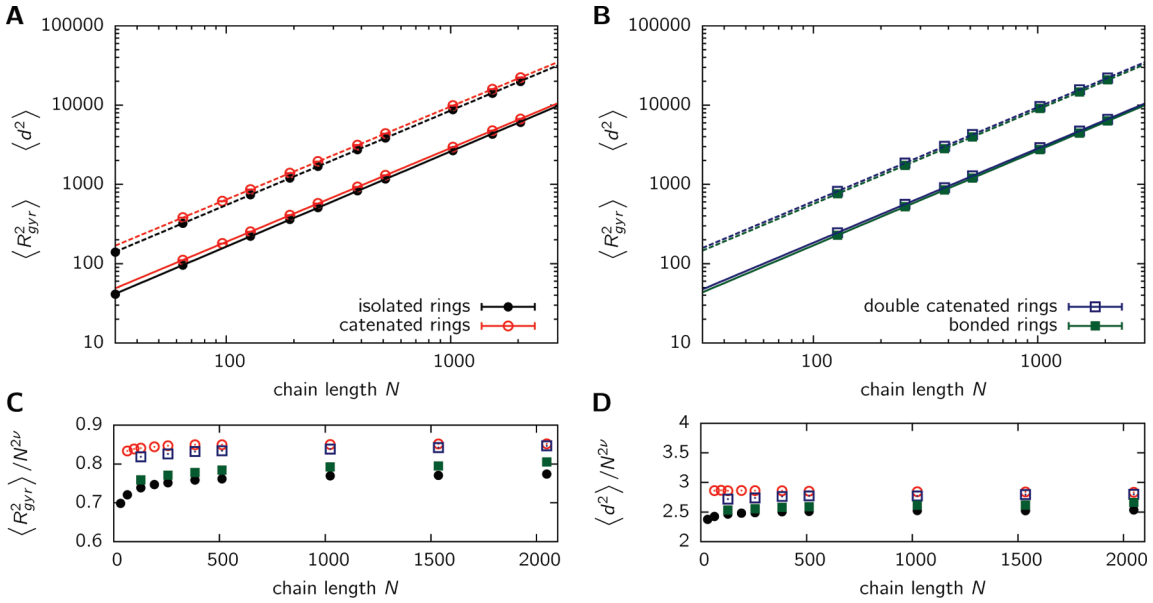

Figure 2. (A,B) Log−log plots of the mean-squared radius of gyration $\langle R_{gyr}^2 \rangle$ (solid line) and the mean square ring diameter $\langle d^2 \rangle$ (dashed line) in dependence of chain length, N. Results are presented for isolated rings (●), single catenated rings (○), double-catenated rings (□), and noncatenated bonded rings (■); separation in two figures is done for reasons of readability. Lines represent a fit to the scaling law $\langle \cdot \rangle = b^2 N^{2\nu}$. (C,D) Mean-squared radius of gyration $\langle R_{gyr}^2 \rangle$ and ring diameter $\langle d^2 \rangle$ with the leading order term $N^{2\nu}$ of the self-avoiding walk behavior $\nu = 0.588$ divided out. In all cases, standard errors are smaller than the point size.

Instead, one can characterize the dimensions of a ring polymer by the mean square ring diameter $\langle d^2 \rangle$, which is defined by the average squared distance between two monomers separated by $N/2$ monomers along the contour of the chain

$$\langle d^2 \rangle = \frac{1}{|\mathcal{C}|} \frac{1}{N} \sum_{c \in \mathcal{C}} \sum_{i=1}^{N} \| \mathbf{r}_{i+N/2}^c - \mathbf{r}_i^c \|^2$$

Here $\mathcal{C}$ denotes the set of sampled conformations, and $\mathbf{r}_i^c$ denote the coordinates of the i^{th} monomer in conformation $c \in \mathcal{C}$. Furthermore, the radius of gyration $\langle R_{gyr}^2 \rangle$ can be used as a characterization of the length scale, both for rings as well as self-avoiding walks.

It has been shown in several studies, that isolated self-avoiding ring polymers follow a similar scaling law as linear polymers both for the radius of gyration $\langle R_{gyr}^2 \rangle$ as well as for the ring diameter $\langle d^2 \rangle$

$$\langle R_{gyr}^2 \rangle_i \approx N^{2\nu} \quad \langle d^2 \rangle_i \approx N^{2\nu}$$

The index i denotes an average over the ensemble of isolated chains. Sikorski[27] determined the scaling exponent for the radius of gyration to $\nu = 0.587$. Similar results were found by Brown et al.[13] ($\nu = 0.585$) and Müller et al.[14] ($\nu = 0.595$). The exponents for the mean square ring diameter are differing only slightly in these studies: $\nu = 0.59$ (Sikorski), 0.585 (Brown), and 0.605 (Müller). Within the errors of the simulations, these results show that isolated polymer rings have the same scaling exponent as linear self-avoiding polymers.

Furthermore, Sikorski in his paper[27] analyzed these quantities for one ring concatenated with a second ring. His data show that even catenated rings ($\Phi = 1$) obey a scaling law with scaling exponents $\nu = 0.591 \pm 0.002$ for the radius of gyration and $\nu = 0.587 \pm 0.002$ for the ring diameter, suggesting that the scaling exponents are equal within the statistical errors. However, an analysis for the limit $N \to \infty$ has not been performed.

Table 1. Scaling Exponents, ν, for the Mean-Squared Radius of Gyration and Ring Diameter[a]

type	ν_1	ν_2
isolated	0.601(1)	0.596(1)
catenated	0.592(1)	0.5871(3)
double-catenated	0.594(1)	0.594(1)
bonded	0.598(1)	0.595(1)

[a] Scaling exponents have been determined by a fit to $\langle R_{gyr}^2 \rangle = b^2 N^{2\nu_1}$ and $\langle d^2 \rangle = b^2 N^{2\nu_2}$ using the least-squares algorithm. Errors represent the asymptotic standard error of the fit.

Here we determine the scaling exponents, ν, for the above-mentioned topologies and carry out a finite-size analysis to see whether the scaling exponents differ in the limit of infinite chain length N. Figure 2A,B shows the radius of gyration $\langle R_{gyr}^2 \rangle$ and the ring diameter $\langle d^2 \rangle$ for chains of length up to $N = 2048$ in a logarithmic plot. Consistent with other studies, we find exponents of $\nu = 0.601(1)$ for the radius of gyration and $\nu = 0.596(1)$ for the mean square ring diameter of single rings. For simple catenated rings, parameter fitting yields $\nu = 0.592(1)$ for the radius of gyration and $\nu = 0.5871(3)$ for the ring diameter. Error estimates of the fitting parameters are based on the asymptotic standard errors resulting from a least-squares fit using the gnuplot software (version 4.2). Scaling exponents including other topologies are summarized in Table 1.

It has been shown[16] that the topological constraint of noncatenation induces a change in the scaling law from the self-avoiding walk to a globular state in a melt of polymers. To analyze whether the scaling exponents of a ring linked or bonded to a second ring is actually equal in the limit of large chains, we analyze the swelling factor $s = \langle R_{gyr}^2 \rangle_t / \langle R_{gyr}^2 \rangle_i$. Here $\langle \cdot \rangle_i$ denotes an average over the ensemble of isolated rings, whereas $\langle \cdot \rangle_t$ designates the ensemble average over one of the two-ring topologies, that is, catenated ($\Phi = 1$), double-catenated ($\Phi = 2$), or bonded ($\Phi = 0$). In the case of the scaling exponents being unequal, the swelling factor would scale with $s \approx N^{\delta\nu}$, $\delta\nu > 0$, thus displaying either convergence to zero or divergence to infinity in the

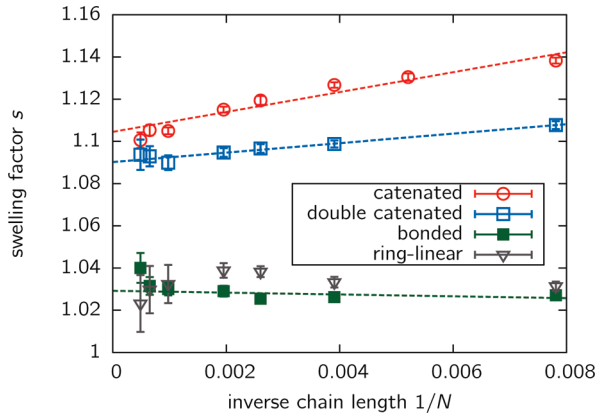

Figure 3. Swelling factor $s = \langle R^2_{\mathrm{gyr}}\rangle_t/\langle R^2_{\mathrm{gyr}}\rangle_i$ between the mean-squared radius of gyration of a ring topologically constrained to a second ring (index t) and isolated rings (index i). The Figure reveals that catenated rings forming the Hopf link and double-catenated rings are more swollen compared with isolated chains by ∼10%, the effect being smaller but existent for bonded rings. Data is plotted versus the inverse chain length $1/N$ to allow for an extrapolation to $N \to \infty$. Such an extrapolation results in finite values of the swelling factor, s, indicating that the scaling exponents of isolated rings and rings within a two-chain system display the same scaling exponent.

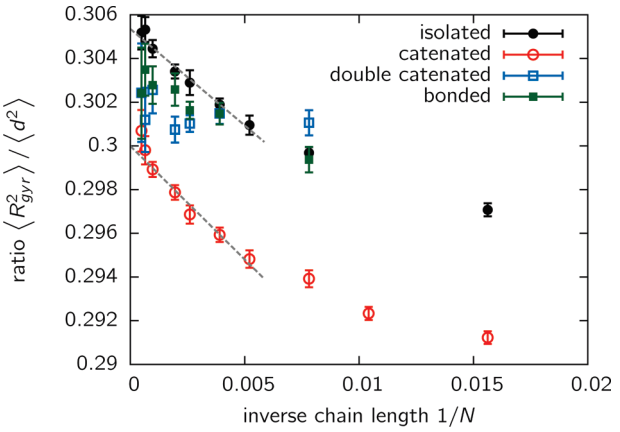

Figure 4. Ratio $\langle R^2_{\mathrm{gyr}}\rangle/\langle d^2\rangle$ between radius of gyration and the mean square ring diameter for the ring topologies under study. For isolated and catenated rings (linking number $\Phi = 1$), the ratio reaches an asymptotic value in the limit of large chains ($N \to \infty$) determined by a crude linear extrapolation to $\langle R^2_{\mathrm{gyr}}\rangle_i/\langle d^2\rangle_i = 0.3053(2)$ and $\langle R^2_{\mathrm{gyr}}\rangle_c/\langle d^2\rangle_c = 0.2995(3)$. Results for double-catenated rings (linking number $\Phi = 2$) and bonded rings display too large fluctuations to conduct a reasonable fit.

limit $N \to \infty$. The swelling factor is shown in Figure 3 versus the inverse chain length to allow for an easy extrapolation. We find that for all two-ring topologies studied, the swelling factor, s, adopts a constant and finite value in the limit of large chain lengths. Clearly, no divergence to infinity or convergence to zero can be found. To obtain an estimate for the swelling factor in the large chain limit, we perform a crude linear extrapolation assuming that first-order finite-size corrections scale as $s \approx \mathcal{O}(1/N)$. We find that catenated and double-catenated rings are swollen by a factor of ∼10% compared with isolated chains (catenated rings: $s = 1.105(2)$, double-catenated rings: $s = 1.090(1)$). Bonded rings are smaller, their size being only ∼3% larger than that of isolated rings ($s = 1.028(2)$).

We conclude that changes in dimensionality are not as drastic by the introduction of topological constraints as a different scaling exponent would induce. Nevertheless, the effective segment length, b (the prefactor of the scaling law), becomes larger in the presence of a second ring, and thus the ring is swollen by a constant factor in comparison with isolated chains. Comparison of the swelling factor, s, for bonded rings and the corresponding ring-linear system indicates that the swelling is due to the extra material in vicinity rather than topological constraints.

Scaling considerations suggest that both the radius of gyration and the mean square ring diameter have to follow the same scaling law: There is only one length scale involved in the system, which is parametrized by the chain length and the bond length. Therefore, the scaling exponent, ν, has to be equal for both quantities. This can be validated by looking at the ratio of radius of gyration to mean square ring diameter $\mathcal{R} \equiv \langle R^2_{\mathrm{gyr}}\rangle/\langle d^2\rangle$. The complementary quantities for linear chains are the radius of gyration and the end-to-end distance; here the ratio $\langle R^2_{\mathrm{gyr}}\rangle/\langle R^2_{\mathrm{e}}\rangle$ is a constant, which turns out to be equal to $^1/_6$ for both the random walk as well as the self-avoiding walk polymer model.[34] The ratios $\mathcal{R}$ for single and catenated rings are shown in Figure 4. Deviations from a constant value are most probably due to finite-size effects, as we find $\mathcal{R}(N) \to$ const. ($N \to \infty$) for both single and catenated rings. Although we do not know how to correct this quantity for finite-size effects, for large chain length ($N > 256$), corrections to the limiting case seem to be on the order of $\mathcal{R}(1/N)$. Linear regression yields the ratios $\mathcal{R}(N \to \infty) = 0.3053(2)$ for isolated rings and $\mathcal{R}(N \to \infty) = 0.2995(3)$ for catenated rings. Extrapolation for double-catenated and bonded rings is more difficult because the data show more fluctuations; the ratios are, however, bounded by the values for isolated and catenated rings.

Shape of Ring Polymers Changes Due to Topological Constraints. In the last section, there has been given evidence that the dimensions of a ring polymer constrained to another using the topologies in Figure 1 change only with respect to the effective segment length b and not to the scaling exponent ν compared to an isolated ring, leading only to a mild swelling of the polymer (by a factor of up to 1.10) even in the limit of very large chains. Here we want to analyze how the existence of a second ring catenated or bonded to it influences the shape of this polymer. It is common to describe the shape properties of a ring by means of the gyration tensor.[35,36] This quantity, represented as a 3×3 matrix, describes the distribution of points in space and is defined by

$$S_{mn} = \frac{1}{N}\sum_{i=1}^{N} r_m^{(i)} r_n^{(i)} \qquad (3)$$

Here $\mathbf{r}^{(i)}$ is the coordinate vector of the ith monomer, and the subindex denotes its Cartesian components. The matrix $\mathbf{S}$ is symmetric and positive semidefinite, and thus it can be transformed to a diagonal matrix where the three eigenvalues $\lambda_1 \le \lambda_2 \le \lambda_3$ give the squared lengths of the principal axes of gyration of the associated gyration ellipsoid. The shape of the ellipsoid resembles the distribution of masses of the monomer containing the monomer coordinates only in a summarized way, therefore allowing comparison between different conformations.

The ratios of the eigenvalues $\langle\lambda_3\rangle/\langle\lambda_1\rangle$ and $\langle\lambda_2\rangle/\langle\lambda_1\rangle$ indicate the deviation from a spherelike shape of the polymer, both having a value of unity for a sphere. It is well-known that individual linear polymer chains display a pronounced asphericity, which shows up in the asymptotic ratios of the eigenvalues, namely[37]

$$\langle\lambda_3\rangle : \langle\lambda_2\rangle : \langle\lambda_1\rangle \to 12 : 2.7 : 1 \quad \text{(random walk)}$$

$$\langle\lambda_3\rangle : \langle\lambda_2\rangle : \langle\lambda_1\rangle \to 14 : 2.98 : 1 \quad \text{(self-avoiding walk)}$$

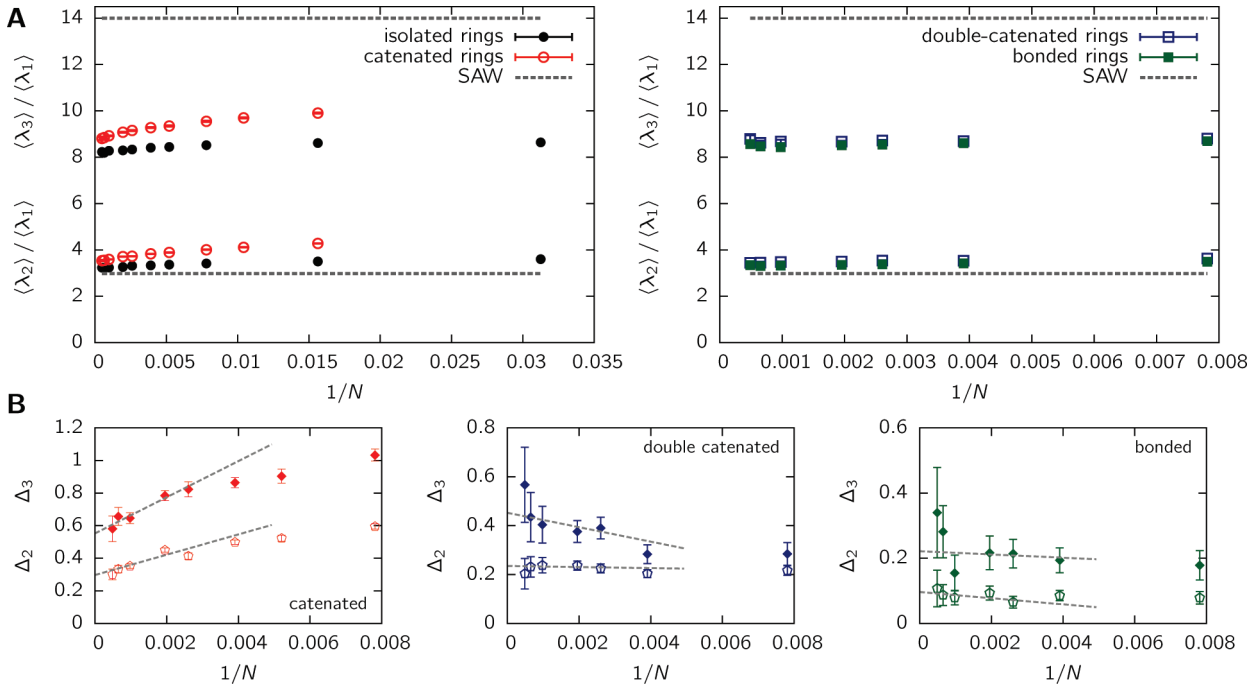

Figure 5. (A) Ratios of the average eigenvalues $\langle\lambda_3\rangle/\langle\lambda_1\rangle$ and $\langle\lambda_2\rangle/\langle\lambda_1\rangle$ of the gyration tensor for single (●) rings, catenated rings (○, linking number $\Phi = 1$), double-catenated rings (□, linking number $\Phi = 2$), and rings bonded to each other (■). Ratios show distinct differences from linear chains (self-avoiding walk, dashed gray line), however, differences between isolated rings and rings catenated or bonded to a second one are more subtle. (B) This panel shows the difference between the eigenvalue ratios of a ring in a two-chain conformation and isolated rings $\Delta_k = \langle\lambda_k\rangle_t/\langle\lambda_1\rangle_t - \langle\lambda_k\rangle_i/\langle\lambda_1\rangle_i$ ($k = 2, 3$): ◆, Δ_3; ◇, Δ_2. The plots reveal that the shape of isolated and catenated or bonded rings is different, even in the limit of infinite chains.

We determined the eigenvalue ratios for isolated, simple, and double-catenated ring polymers and bonded ring polymers in dependency of its chain length. Results in Figure 5A clearly show that isolated ring polymers are more spherical than their linear counterparts, in agreement with simulations in ref 6, In fact, this result does not come as a big surprise: One would recover the linear chain result if the ring was collapsed to a linear polymer with two strands aligned parallel to each other. However, this is only one possible conformation, and the ring has many more entropic degrees of freedom, all of them having a less-pronounced asymmetry. Whereas the deviations between self-avoiding walks and rings are large concerning the elongation of the polymer, differences in the shape of isolated rings and the two-ring topologies studied are more subtle. In fact, we find differences between isolated rings compared with their counterparts in a two-ring system; the question of whether these differences remain in the infinite chain limit, however, cannot be answered from Figure 5A. Therefore, a thorough extrapolation to the infinite chain limit is conducted in Figure 5B for the three topologies under investigation. The Figures show the difference in the eigenvalue ratios compared with the isolated case

$$\Delta_k \equiv \langle\lambda_k\rangle_t/\langle\lambda_1\rangle_t - \langle\lambda_k\rangle_i/\langle\lambda_1\rangle_i \quad (k = 2, 3)$$

Data are plotted against the inverse chain length $1/N$ to allow for an extrapolation to the infinite chain limit. Linear extrapolation to $N \to \infty$ indeed indicates that the difference does not vanish for either of the topologies studied, and hence the shape of an isolated ring is significantly different from that of a ring topologically constrained to another.

A crude linear extrapolation of the eigenvalue ratios for single rings yields

$$\langle\lambda_3\rangle/\langle\lambda_1\rangle \to 8.23 \pm 0.02 \quad (N \to \infty) \tag{4}$$

$$\langle\lambda_2\rangle/\langle\lambda_1\rangle \to 3.22 \pm 0.02 \quad (N \to \infty) \tag{5}$$

These results differ slightly from data of Bishop et al.,[6] where ratios of 7.76:3.10:1.00 were reported for isolated rings with excluded volume. Although this study applied off-lattice simulations, the maximum chain length, $N = 64$, might still be in a regime where finite-size effects are observable.

For catenated rings with linking number $\Phi = 1$, we obtain the ratios

$$\langle\lambda_3\rangle : \langle\lambda_2\rangle : \langle\lambda_1\rangle \to 8.87(3) : 3.56(2) : 1$$

A list with the ratios for double-catenated rings and bonded rings is given in Table 2.

Other publications[35,38] use different measures for the shape of the gyration tensor. Two of these measures are the asphericity, A, and the prolateness, P. The asphericity value displays deviations from the spherelike shape of the polymer and is defined by

$$A(\lambda_1, \lambda_2, \lambda_3) = \frac{(\lambda_1 - \lambda_2)^2 + (\lambda_1 - \lambda_3)^2 + (\lambda_2 - \lambda_3)^2}{2(\lambda_1 + \lambda_2 + \lambda_3)^2}$$

For a rodlike shape of the gyration ellipsoid, we find $A = 1$, whereas for a spherelike shape, $A = 0$. The prolateness is given by

$$P(\lambda_1, \lambda_2, \lambda_3) = \frac{(2\lambda_1 - \lambda_2 - \lambda_3)(2\lambda_2 - \lambda_1 - \lambda_3)(2\lambda_3 - \lambda_1 - \lambda_2)}{2(\lambda_1^2 + \lambda_2^2 + \lambda_3^2 - \lambda_1\lambda_2 - \lambda_1\lambda_3 - \lambda_2\lambda_3)^{3/2}}$$

A positive value of P indicates a prolate shape of the gyration ellipsoid, and a negative value indicates an oblate shape.

Prolateness and asphericity for isolated and simple catenated rings with up to $N = 2048$ monomers are shown in Figure 6. We find that the asphericity is larger for catenated rings than for isolated rings, even in the limit of infinite chain length. Extrapolation to $N \to \infty$ yields $A = 0.2559 \pm 0.0003$ for single rings and $A = 0.2602 \pm 0.0003$ for catenated rings.

Table 2. Shape of Ring Polymers[a]

type	$\langle\lambda_3\rangle:\langle\lambda_2\rangle:\langle\lambda_1\rangle$	A	P
isolated	8.23(2):3.22(2):1	0.2559(3)	0.451(2)
catenated	8.87(3):3.56(2):1	0.2602(3)	0.416(3)
double-catenated	8.66(2):3.46(1):1	0.258(1)	0.424(3)
bonded	8.46(2):3.31(1):1	0.2592(3)	0.416(2)

[a] Shape is characterized by the asphericity, A, prolateness, P, and the eigenvalue ratios, $\langle\lambda_3\rangle:\langle\lambda_2\rangle:\langle\lambda_1\rangle$, of the gyration tensor extrapolated to $N \rightarrow \infty$. Extrapolation has been conducted by a linear fit to the data displayed in Figure 5A for chains longer than $N = 128$. Fitting was done using the least-squares algorithm in gnuplot (version 4.2); errors indicate the asymptotic standard error of the fit.

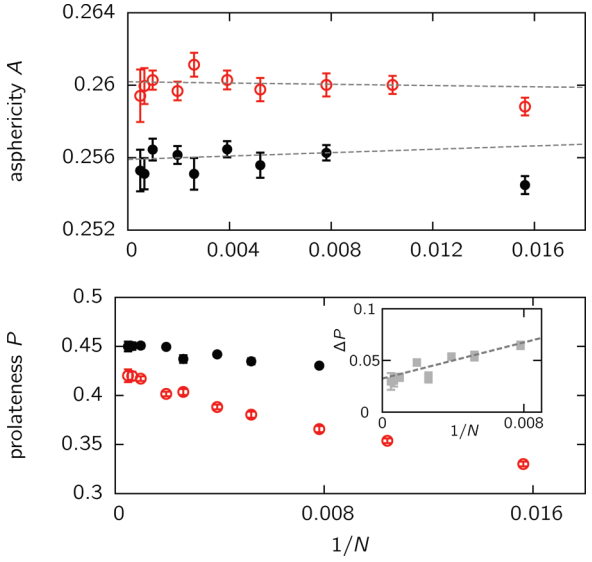

Figure 6. Asphericity, A, and prolateness, P, for single and catenated ring polymers. Data are plotted against the inverse chain length, $1/N$, to allow for extracting the asymptotic limit, $N \rightarrow \infty$: ●, isolated rings; ○, simple catenated rings. The inset shows the difference in the prolateness, P, between single and catenated rings in relation to inverse chain length, $1/N$. The difference does not vanish for infinite chain length, and thus prolateness between isolated and catenated rings is systematically different.

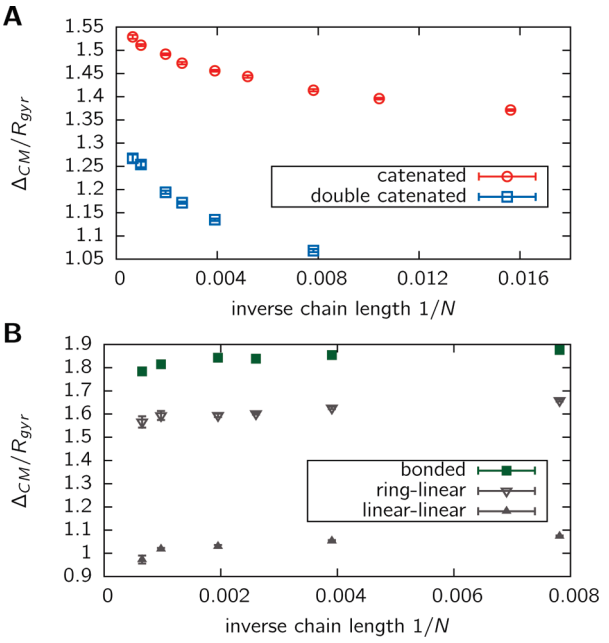

Figure 7. (A) Influence of the catenation constraints with linking number $\Phi = 1,2$ on the average distance Δ_{CM} between the centers of mass. Shown is data for rings with a single link and a double link versus inverse chain length. The distances are given relative to the radius of gyration $R_{gyr} = (\langle R_{gyr}^2\rangle)^{1/2}$ of one ring. Data show that the two rings have a tendency to segregate, which becomes stronger for larger chains. (B) Influence of the ring shape on noncatenated polymers bonded to each other. Shown is the average distance between the centers of mass in relation to inverse chain length for a system consisting of two rings (■), a ring bonded to a linear polymer (△), and two linear chains (▲). Data are scaled with the radius of gyration of one ring (or one linear chain in case of the linear−linear system). Segregation is markedly stronger for the system consisting of two rings.

The result for single rings is in agreement with earlier studies.[35,38] The prolateness is smaller for catenated rings, but the inset of Figure 6 shows that differences remain even in the limit $N \rightarrow \infty$. Linear extrapolation to $N \rightarrow \infty$ yields $P = 0.451 \pm 0.002$ for isolated rings and $P = 0.416 \pm 0.0003$ for catenated rings. The values for other topologies are displayed in Table 2.

Ring Structure Induces Entropy-Driven Segregation. Of major interest concerning the benefit of loop formation in proteins, DNA, or chromatin is the influence of the imposed topological constraint on the relative positioning of the two polymers, that is, the entropic effect of the ring structure. Catenation, for example, sets a constraint on the maximal distance between the centers of mass of the two rings. Intuitively, a large center-of-mass separation strongly restricts the number of accessible conformations and therefore seems entropically unfavorable. A complete mixing of both rings might be possible, which would also agree with the finding that catenated rings are swollen compared with isolated ones. Similar behavior can be expected in case of noncatenated rings bonded to each other.

Information about the segregation of the two ring polymers is given by the average distance between the centers of mass of both rings. Let $R_{gyr} = (\langle R_{gyr}^2\rangle)^{1/2}$ be the root-mean-squared radius of gyration of ring 1. The radius of gyration tells us the average distance that two randomly chosen monomers on ring 1 have. If the chains intermingle completely, then the average distance between the centers of mass, Δ_{CM}, given in units of the radius of gyration should be equal to unity. However, if the rings tend to segregate, then this quantity should be above unity. We first looked at this quantity with respect to the constraint of catenation for both the case of the Hopf link ($\Phi = 1$) and the case of linking number $\Phi = 2$. We find from Figure 7A that the center of mass, $\mathbf{r}_{CM}^1$, of ring 1 is indeed positioned more distant than one radius of gyration, R_{gyr}, from that of ring 2. Therefore, the two rings are not completely overlapping but segregate to some extent. This tendency becomes even stronger the larger the chain length, N. The question of whether the normalized distance approaches a constant value or diverges to infinity cannot be answered from the data. Increasing the linking number between two ring polymers forces them to be closer together, and thus double-catenated rings display a smaller center-of-mass separation in relation to size (Figure 7A), which however shows a steep ascent in the long chain limit. These findings can be explained well by entropy-driven segregation because of the fixed catenation topology. Consider two phantom ring polymers, which are brought in close proximity. The probability of having a large linking number increases with chain length. Therefore, the probability for linking numbers 1 and 2 decreases, making short center-of-mass separations unlikely in the ensemble constrained to simple catenation or double-catenation.

The biological problem of chromatin folding and the effect of chromatin loops on segregation can be investigated most clearly by looking at the noncatenated bonded topology

(Figure 1D). To highlight the effect of loops, we compare this system with both the case of a linear polymer bonded to a ring (Figure 1E) and two linear polymers bonded to each other at the center monomer (Figure 1F). The center-of-mass separation is shown in Figure 7B. As in the case of catenated rings, the center-of-mass distance is scaled with the radius of gyration, R_{gyr}, of one single ring in the case of the linear−linear system with the radius of gyration of one linear chain. We find that the segregation of the ring−ring system is much stronger than the ring−linear and linear−linear systems. The two last mentioned systems do not have the noncatenation constraints; that is, the accessible configurational space is larger at short center-of-mass separations. In fact, the linear−linear system shows almost complete intermingling, with the center-of-mass separation being close to the radius of gyration of a single chain. A general conclusion emerging from these results is that topological constraints imposed by looping, that is, the noncatenation constraint, play a dominant role in driving the segregation of close-by loops. Therefore, a kind of order is induced in the system, which cannot be accomplished by linear polymers.

By projecting the monomers to the line connecting the centers of mass, we can determine the density distribution of monomers of both chains along this line, displaying the degree of intermingling or overlap. Figure 8A shows the projected line density of monomers for a system of two catenated ring polymers along the vector connecting the centers of mass. The data are evaluated in units of the center of mass distance, the origin being halfway between the centers of mass. The Figure shows that the polymer rings are indeed well separated. Interestingly, as the curves for $N = 128$ and 1024 show, the overlap area decreases with chain length. This overlap area of the two curves in Figure 8A is plotted against the chain length in Figure 8B for the catenated systems studied. We find that the overlap area decreases with N and reaches a constant value in the limit of $N \rightarrow \infty$ for rings with one or two links.

Importantly, such a separation of density clouds is mediated by the looping. This can be seen most clearly by comparing two bonded rings with the corresponding ring−linear and linear−linear systems (Figure 8C). We find that the overlap area of the monomer density distributions is significantly smaller in case of two bonded ring polymers compared with systems with linear polymers.

Alignment of Ring Polymers. Of interest concerning the segregation of monomers is not only the center-of-mass distance but also the alignment of the two rings with respect to each other. Again, we turn to the gyration ellipsoid, which yields direct information about the distribution of masses in space. In particular, we study the orientation of the longest principal axes of the gyration tensors with respect to each other. For this purpose, we analyze the average angle $\langle \cos \theta \rangle$ between these axes. Because they are bidirectional, they force the angle θ to be in the interval $[0, \pi/2]$. We find that the gyration tensors are not independently oriented with respect to each other, which would correspond to an average angle between the main axes of $\langle \cos \theta \rangle = 0.5$. In fact, the gyration ellipsoids tend to collocate in a more perpendicular orientation (Figure 9) for all two-ring topologies studied. Linear extrapolation to $N \rightarrow \infty$ yields $\langle \cos \theta \rangle = 0.466(1)$ ($\theta \approx 62.2°$) for catenated rings, $\langle \cos \theta \rangle = 0.477(1)$ ($\theta \approx 61.5°$) for double-catenated rings, and $\langle \cos \theta \rangle = 0.491(2)$ ($\theta \approx 60.6°$) for bonded rings. Intuitively, one could expect that if there is a repulsion between the two rings due to excluded volume or topological constraints, then the gyration ellipsoids would try to align in the same orientation and separate their centers of mass so that the gyration ellipsoids do not overlap.

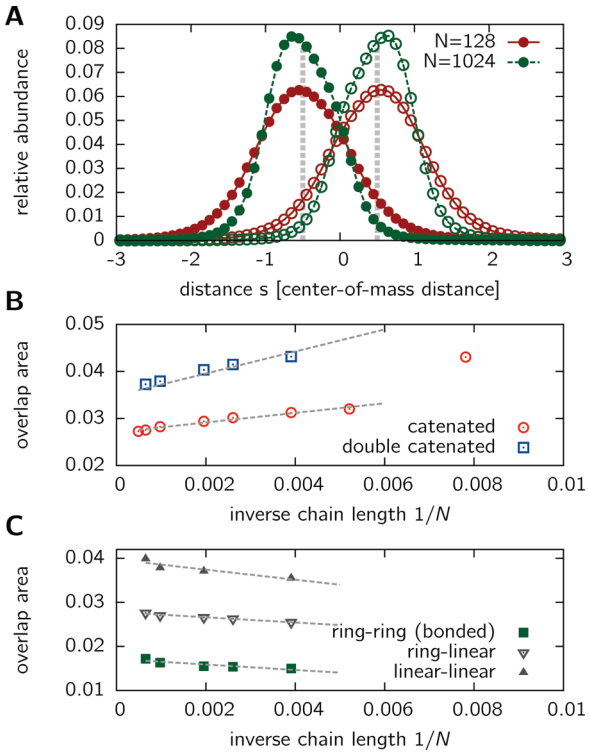

Figure 8. (A) Distributions of monomers projected onto the line connecting the centers of mass of two catenated rings (linking number 1). The data show the relative abundance of projected monomer positions of both rings with respect to the axis between the centers of mass. The scale on the x axis is given in units of the center-of-mass distance. The origin corresponds to the point in between the centers of mass, and the gray vertical lines represent the positions of the centers of mass. Data show that monomer clouds of both rings are rather separated. (B) Overlap area in the graphs of the projected monomer distributions as displayed in A for catenated (linking number 1) and double-catenated rings (linking number 2). This overlap area decreases approximately linearly, with inverse chain length reaching asymptotically a constant value. (C) Overlap area of projected monomer distributions for a system of two noncatenated polymers, which at their centers are bonded. The existence of rings markedly decreases the overlap.

However, it seems that this is entropically very unfavorable because of the catenation or bonding constraint, which prohibits a large separation of the centers of mass. Therefore, if there is an entropic barrier preventing segregation and forcing the gyration tensors to overlap, then the perpendicular orientation minimizes the overlap area. This is exactly what we observe. Furthermore, the more perpendicular orientation makes the complete system more sphere-shaped and thus more symmetric. In agreement with this is our finding that the angle, θ_{CM}, between the vector connecting the centers of mass and the largest principal axis of the gyration tensor of a ring is slightly smaller than that expected from a random orientation of both vectors. Extrapolation of $\langle \cos \theta_{CM} \rangle$ yields values of 0.580(1), 0.586(1), and 0.566(1) for simple catenated, double-catenated and bonded rings, respectively. Figure 9B shows a typical conformation out of the ensemble of simple catenated two-ring conformations. Both the alignment of the gyration ellipsoids as well as the aspherical shape are visible.

To analyze the orientations of the gyration tensor in more detail, we investigated its orientation in dependence of the center of mass separation. The average angle $\langle \cos \theta \rangle$ between the two largest principal axes of the gyration ellipsoids is shown in Figure 10 for simple and double-catenated rings. The closer the centers of mass are, the more perpendicular

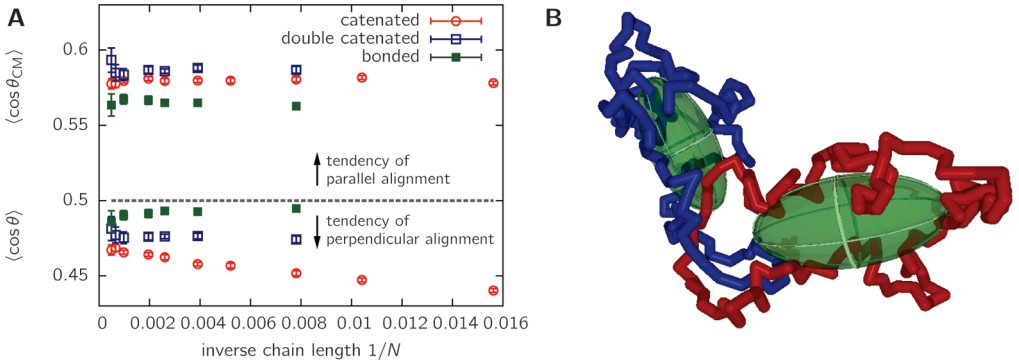

Figure 9. A. Alignment of the gyration ellipsoids with respect to each other. Data at the bottom displays the average angle $\langle \cos \theta \rangle$ between the two largest principal axes of the gyration ellipsoid. Data at the top represents the average angle $\langle \cos \theta_{CM} \rangle$ between the largest principal axis of one ring and the vector connecting the centers of mass. The gray line corresponds to the average orientation in the case of both vectors having a random orientation. The gyration ellipsoids of all topologies studied align on average more perpendicularly than expected by random orientation, while their alignment w.r.t the center of mass connecting vector tends to be parallel B. One conformation consisting of two catenated rings and its gyration ellipsoids drawn out of the ensemble. The example conformation visualizes (i) the segregation of the two rings (the ellipsoids are well separated), (ii) the aspherical shape of the gyration ellipsoids and (iii) their perpendicular alignment.

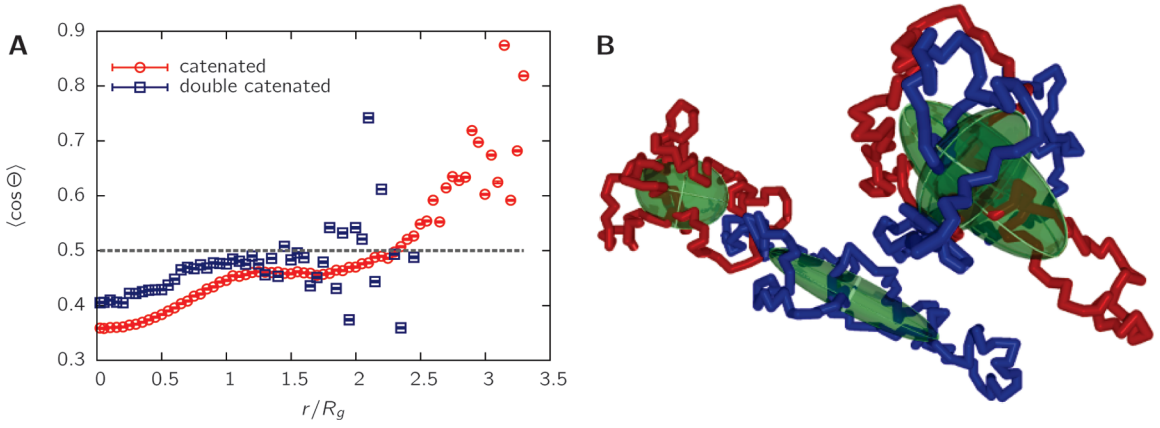

Figure 10. (A) Orientation of the gyration ellipsoids in dependence of CM separation. Shown is the average angle $\langle \cos \theta \rangle$ between the largest principal axes of the gyration ellipsoid of both simple catenated rings (linking number 1) and double-catenated rings (linking number 2) in dependence of their center-of-mass distance. The chain length is $N = 1024$. At small separations, the alignment is preferably perpendicular, whereas for large separations, alignment becomes more and more parallel. (B) Two conformations with different center-of-mass separation and simple catenation. The left catenated rings have a CM separation of $r = 3.11R_g$, and the right catenated rings have a CM separation of $r = 0.13R_g$.

the ellipsoids. For large separations, the orientation approaches a parallel alignment: The centers of mass are separated to such an extent that the gyration tensors have to align in a row in the same direction because of the catenation constraint. For double-catenated rings, the tendency is not so clear because of insufficient statistics: a linking number of two becomes very unlikely for large separations. Simple catenated rings display a point at intermediate distances $r \approx 2R_g$ where the two driving forces, minimization of overlap and catenation constraint, are in balance such that the average angle is close to the random orientation value.

Conclusions

In this article, we have studied the influence of topological catenation and bonding constraints on the conformational properties of ring polymers. Three different topologies were studied: simple catenated rings (linking number 1), double-catenated rings (linking number 2), and noncatenated bonded rings. In particular, we were interested in the question of whether the dimensions and the shape change compared with isolated rings. More importantly, we investigated the positioning and alignment of the two rings with respect to each other to detect whether there is an entropic repulsion that can lead to a segregation of the polymers.

We find that the size of a ring topologically constrained to another ring is more swollen compared with isolated rings, the swelling factor in the infinite chain limit $N \rightarrow \infty$ being about 1.10 for catenanes and 1.03 for bonded rings (Figure 3). However no indication was found in the regime of chain lengths studied here that the scaling exponents are different from the case isolated rings, where the scaling exponent is close to the self-avoiding walk value of $\nu \approx 0.588$.

Whereas dimensions of the ring polymers only change by a constant factor, the effective bond length, b, and the shape of catenated or bonded rings differ substantially, a finding that is in contrast with the conjecture put forward by Sikorski.[27] This is shown for the ratios of the gyration tensors eigenvalues (Figure 5). These ratios are generally smaller for rings compared with their linear counterparts, the shape being still markedly prolate. However, the prolongation is stronger for a catenated or bonded ring than for isolated rings (Table 2). This difference also shows up in the measures of asphericity, A, and prolateness, P, which are commonly used shape parameters.[35]

The change in the shape of one ring in the system of two topologically constrained rings already indicates an entropic effect of the fixed topology. We have analyzed whether rings tend to segregate, arranging themselves into distinct spatial territories, or if they can intermingle freely. We found that for catenanes with small linking numbers, there is a strong tendency

toward segregation, which shows up in the separation of the centers of mass compared with the radius of gyration of a single chain (Figure 7A) and in the density distribution of monomers along the center of mass (Figure 8A). The segregation is even more pronounced for longer chains driven by the tendency to create more complicated links at short separations. Interestingly, noncatenated bonded rings show a markedly stronger segregation than bonded linear chains, revealing the importance of the ring closure on segregation. These effects also become visible in the alignment of the gyration ellipsoids. We found a tendency to align more perpendicular than expected from a random orientation (Figure 9). Presumably, such an orientation minimizes the overlap between the monomers of different chains and bypasses the prohibited formation of more complicated links. Because a large center-of-mass separation is entropically unfavorable and therefore the chains have to stay quite close, the perpendicular alignment has a smaller overlap volume than a parallel alignment.

The findings of this study have several biological implications for catenated DNA[21] and proteins.[22] Similar effects might be expected for chromatin folding, although the chromatin fiber has a much more complex topology.[5,39] Generally speaking, simple and double-catenated polymers adopt a more aligned and segregated structure. Ring polymers in proximity, which is achieved here by creating a bond between them, have a strong tendency to segregate, inducing a kind of order in the system that cannot be accomplished by linear polymers. It is well-known that compartmentalization is important for maintaining life in higher eukaryotes, both the plasma membrane as well as the nuclear membrane providing such compartments. Although the detailed topology of chromatin is not known, chromatin loops have been shown to play a dominant role in transcriptional regulation.[4] Several studies have indicated a strong effect of looping on the observed segregation of chromosomes, partially studied by a model of ring polymers.[18,19,25] Whereas we would expect the influence of looping to become stronger in the presence of multiple loops, as found in transcription factories,[40] it remains to be shown to what extent the segregation and alignment of ring polymers observed in the present study also apply to a more complex model of chromatin.

Acknowledgment. We thank H. Horner for fruitful discussions. M.B. acknowledges funding from the Landesgraduiertenförderung Baden-Württemberg and partial support by the Heidelberg Graduate School of Mathematical and Computational Methods for the Sciences. O.L. gratefully acknowledges financial support from DAAD, University of Heidelberg, and the Brazilian agency CNPq.

References and Notes

(1) Fiers, W.; Sinsheimer, R. L. *J. Mol. Biol.* **1962**, *5*, 424–434.
(2) Dulbecco, R.; Vogt, M. *Proc. Natl. Acad. Sci. U.S.A.* **1963**, *50*, 236–243.
(3) Weil, R.; Vinograd, J. *Proc. Natl. Acad. Sci. U.S.A.* **1963**, *50*, 730–738.
(4) Fraser, P. *Curr. Opin. Genet. Dev.* **2006**, *16*, 490–495.
(5) Mateos-Langerak, J.; Bohn, M.; de Leeuw, W.; Giromus, O.; Manders, E. M. M.; Verschure, P. J.; Indemans, M. H. G.; Gierman, H. J.; Heermann, D. W.; van Driel, R.; Goetze, S. *Proc. Natl. Acad. Sci. U.S.A.* **2009**, *106*, 3812–3817.
(6) Bishop, M.; Michels, J. P. J. *J. Chem. Phys.* **1985**, *82*, 1059–1061.
(7) Bishop, M.; Saltiel, C. J. *J. Chem. Phys.* **1988**, *88*, 3976–3980.
(8) Deutsch, J. M. *Phys. Rev. E* **1999**, *59*, R2539–R2541.
(9) Baumgartner, A. *J. Chem. Phys.* **1982**, *76*, 4275–4280.
(10) des Cloizeaux, J. *J. Phys., Lett.* **1981**, *42*, 433–436.
(11) Grosberg *Phys. Rev. Lett.* **2000**, *85*, 3858–3861.
(12) Moore, N. T.; Lua, R. C.; Grosberg, A. Y. *Proc. Natl. Acad. Sci. U.S.A.* **2004**, *101*, 13431–13435.
(13) Brown, S.; Lenczycki, T.; Szamel, G. *Phys. Rev. E* **2001**, *63*, 052801.
(14) Müller, M.; Wittmer, J. P.; Cates, M. E. *Phys. Rev. E* **1996**, *53*, 5063–5074.
(15) Cates, M.; Deutsch, J. *J. Phys.* (*Paris*) **1986**, *47*, 2121–2128.
(16) Müller, M.; Wittmer, J. P.; Cates, M. E. *Phys. Rev. E* **2000**, *61*, 4078–4089.
(17) Vettorel, T.; Grosberg, A. Y.; Kremer, K. *Phys. Biol.* **2009**, *6*, 025013.
(18) Dorier, J.; Stasiak, A. *Nucleic Acids Res.* **2009**, *37*, 6316–6322.
(19) Marenduzzo, D.; Orlandini, E. *J. Stat. Mech.: Theory Exp.* **2009**, *2009*, L09002−.
(20) Depew, D. E.; Wang, J. C. *Proc. Natl. Acad. Sci. U.S.A.* **1975**, *72*, 4275–4279.
(21) Vologodskii, A. V.; Zhang, W.; Rybenkov, V. V.; Podtelezhnikov, A. A.; Subramanian, D.; Griffith, J. D.; Cozzarelli, N. R. *Proc. Natl. Acad. Sci. U.S.A.* **2001**, *98*, 3045–3049.
(22) Zhou, H.-X. *J. Am. Chem. Soc.* **2003**, *125*, 9280–9281.
(23) Simonis, M.; Klous, P.; Splinter, E.; Moshkin, Y.; Willemsen, R.; de Wit, E.; van Steensel, B.; de Laat, W. *Nat. Genet.* **2006**, *38*, 1348–1354.
(24) Marenduzzo, D.; Faro-Trindade, I.; Cook, P. R. *Trends Genet.* **2007**, *23*, 126–133.
(25) Cook, P. R.; Marenduzzo, D. *J. Cell Biol.* **2009**, *186*, 825–834.
(26) Otto, M. *J. Phys. A: Math. Gen.* **2004**, *37*, 2881–2893.
(27) Sikorski, A. *Polymer* **1994**, *35*, 3792–3794.
(28) Binder, K.; Heermann, D. W. *Monte Carlo Simulation in Statistical Physics: An Introduction*, 4th ed.; Springer: New York, 2002.
(29) Carmesin, I.; Kremer, K. *Macromolecules* **1988**, *21*, 2819–2823.
(30) Verdier, P. H.; Stockmayer, W. H. *J. Chem. Phys.* **1962**, *36*, 227–235.
(31) Deutsch, H. P.; Binder, K. *J. Chem. Phys.* **1991**, *94*, 2294–2304.
(32) *Monte Carlo and Molecular Dynamics Simulations in Polymer Science*; Binder, K., Ed.; Oxford University Press: New York, 1995.
(33) Sokal, A. Monte Carlo Methods in Statistical Mechanics: Foundations and New Algorithms. In *Functional Integration: Basics and Applications*; DeWitt-Morette, C., Cartier, P., Folacci, A., Eds.; Plenum Press: New York, 1997.
(34) Grosberg, A. Y.; Khokhlov, A. R. *Statistical Physics of Macromolecules*; AIP Press: New York, 1994.
(35) Rawdon, E. J.; Kern, J. C.; Piatek, M.; Plunkett, P.; Stasiak, A.; Millett, K. C. *Macromolecules* **2008**, *41*, 8281–8287.
(36) Bohn, M.; Heermann, D. W. *J. Chem. Phys.* **2009**, *130*, 174901.
(37) Bruns, W. *Makromol. Chem., Theory Simul.* **1992**, *1*, 287–293.
(38) Bishop, M.; Michels, J. P. J. *J. Chem. Phys.* **1986**, *85*, 1074–1076.
(39) Bohn, M.; Heermann, D. W.; van Driel, R. *Phys. Rev. E* **2007**, *76*, 051805.
(40) Fraser, P.; Bickmore, W. *Nature* **2007**, *447*, 413–417.